TROPICAL-EXTRATROPICAL CLOUDBANDS OVER THE SAHARA

With 11 figures and 1 table

IVAN KUHNEL

Zusammenfassung: Tropische-extratropische Wolkenbänder über der Sahara

Die Studie befaßt sich mit der Analyse der grundlegenden klimatologischen Aspekte von tropischen-extratropischen Wolkenbändern über der Sahara sowie deren Vergleich mit ähnlichen Phänomenen im Bereich von Australien. Die Ergebnisse zeigen, daß die Aktivität der Wolkenbänder über der Sahara auf das Winterhalbjahr beschränkt ist. Das Häufigkeitsmaximum ihrer Entwicklung fällt in den Monat März, und es scheint, daß die Stärke ihrer Aktivität vorwiegend von den Luftdruck- und Meerwassertemperatur-Anomalien im nördlichen Atlantik sowie im südwestlichen Indischen Ozean abhängt. Außer einer kleinen typischen Erhöhung ihrer Frequenz 2–4 Monate vor der ENSO-Hauptphase können die Aktivitäten der Wolkenbänder statistisch auch mit anderen Indizes (wie z. B. der Luftdruckanomalie-Differenz zwischen den Stationen Cocos Insel und Martinique, sowie Martinique und Dakar) in Verbindung gebracht werden. Die Resultate deuten weiterhin an, daß während der Periode Januar-März die Aktivität der Wolkenbänder eine typische Schwankung von ungefähr 20 Tagen aufweist. Ein Vergleich der Struktur (sowie der Art und Weise der Entstehung) zwischen den Wolkenbändern über der Sahara und Australien zeigt, daß beide Wolkenbänder zahlreiche Ähnlichkeiten aufweisen. Dennoch sind einige regionale Unterschiede feststellbar, wie z. B. ihre Reaktionszeit auf das Signal der „Southern Oscillation" oder die Periodizität ihrer Entstehung. Weitere charakteristische Merkmale der Wolkenbänder werden erörtert.

1 Introduction

Being located in the descending branch of large-scale HADLEY circulation and dominated by a subtropical high pressure system for most of the year the climate of the Sahara Desert is generally characterised by arid, clear-sky conditions. Occassionally, this overall pattern can change during the northern winter months due to equatorward outbreaks of cold polar air, which, in turn, are sometimes accompanied by development of long tropical-extratropical cloudbands.

These tropical-extratropical cloudbands, hereafter referred to as TECB, tend to form over the eastern half of the North Atlantic Ocean or the western part of North Africa and extend over several thousand kilometers across the Sahara Desert (Fig. 1 a. 2). They represent the channels along which the tropical heat, energy, and moisture propagate into high latitudes in this part of the world. Moreover, these cloudbands are one of the governing factors in inducing anomalous cloudiness, radiation and (to a lesser degree) rainfall conditions over the central Sahara during the winter months.

As the work of DUBIEF and QUENEY (1935), which describes the observation of fast west-east displacement of "false cirrus bands over the Sahara", suggests, some evidence of TECB presence in this region has already been gathered in some early meteorological work. The verification of these observations could later be found in DUBIEF's (1959) map of average cloudiness over Northern Africa, which showed a similarly oriented band of higher cloud cover extending from the Gulf of Sidra to western North Africa (for orientation see Fig. 2 a).

Nevertheless, the first conclusive climatological aspects of these cloudbands were described only after the introduction of meteorological satellites. The cloudiness pattern of DUBIEF was later confirmed by a satellite data based cloudiness study of WINIGER (1975), suggesting that the tropical-extratropical linkage over the Sahara was especially well developed during northern winter and spring. Later, the same phenomenon was described more clearly by FLOHN (1975), who brought the TECB development in connection with equatorward moving upper level troughs and /or the Sahara depression (which forms in the lee of the Atlas mountains; for orientation see Fig. 2 a). These studies were followed by further works, which discussed indirectly other TECB related aspects, like general circulation and cloud structure (e.g. DE FELICE a. VILTARD 1976), injections of tropical moisture into the atmosphere at low latitudes (e.g. CADET a. NNOLI 1987), water vapour trajectories over Northern Africa (e.g. STUCKI 1983), and TECB related rainfall in North Africa (e.g. WINSTANLEY 1970).

A substantial addition to the early TECB climatologies (e.g. ANDERSON a. OLIVER 1970, FLOHN 1975) was the work of THEPENIER (1981), who investigated the TECB distribution in the Northern Hemisphere for the period 1974–1979. Her climatology has been extended globally in a similarly oriented work of

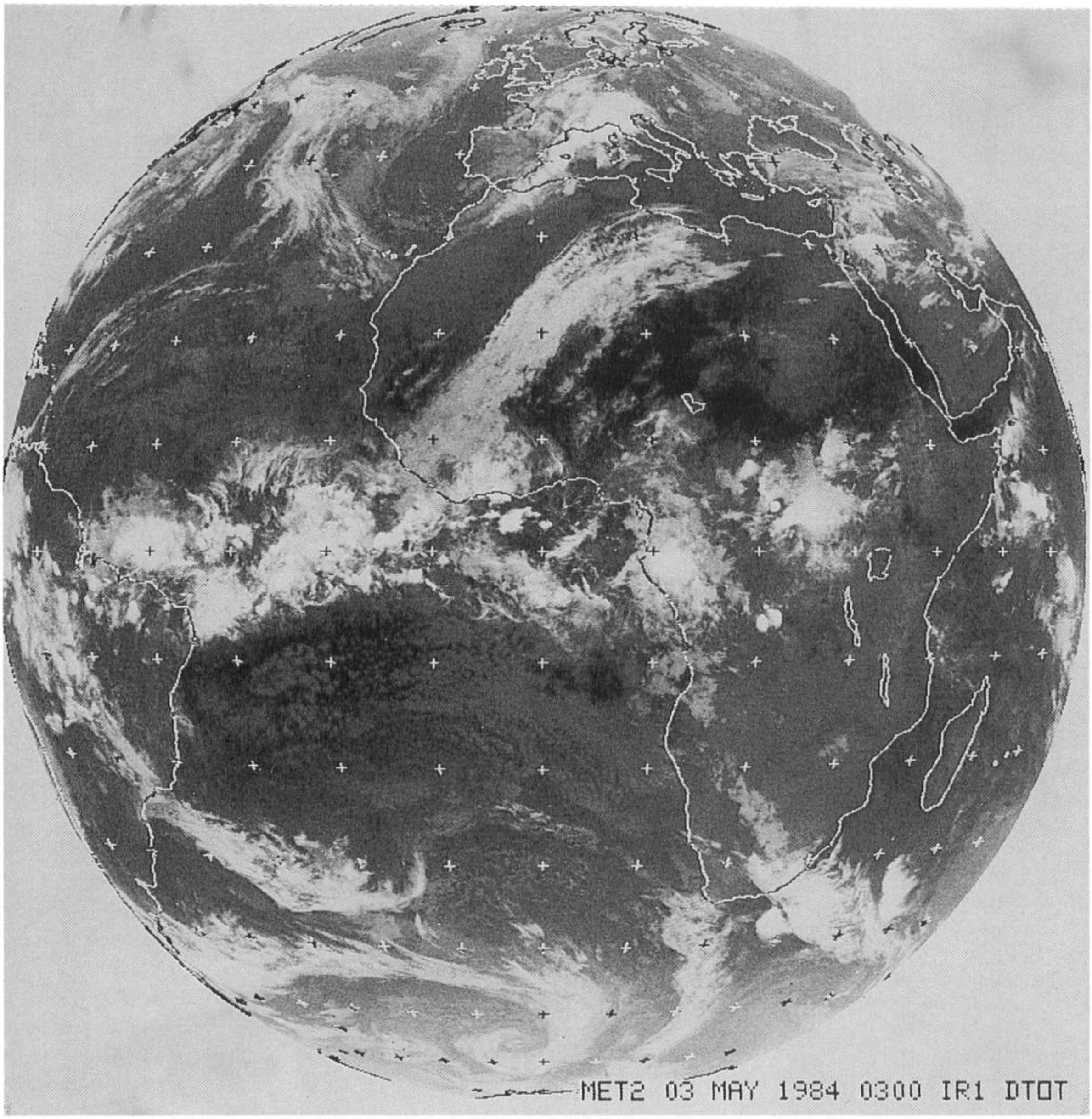

Fig. 1: Infra-red METEOSAT2 imagery from 3 May 1984 0300 GMT, showing a well-developed tropical-extratropical cloudband over the Sahara

Infrarotes METEOSAT2 Bild vom 3. Mai 1984 0300 GMT mit einem gut entwickelten tropischen-extratropischen Wolkenband über der Sahara

KUHNEL (1989). Whereas the results of the latter study put an emphasis on the description of a global TECB distribution, the main objective of this study was a more detailed presentation of the climatology of the TECB over the Sahara. Compilation of such a summary has been considered worthwhile, as, unlike the majority of TECBs (Fig. 4), this cloudband belongs to the very few, whose domain is predominantly of continental character. As the respective part of the North African continent belongs to the most arid and cloudless regions on Earth, the TECB over the Sahara may have a relatively larger climatological importance than other, more active, cloudbands.

In order to keep this study coherent, the first few sections are partly built on information given in KUHNEL (1989), before elaborating on further details. Besides the presentation of TECB frequencies, this study concentrates on a more detailed analysis of possible relationships between the cloudband activity over the Sahara and some meteorological parameters, such as the mean sea level pressure anomalies and sea surface temperature anomalies in the tropics. Furthermore, it investigates possible connections between the cloudband development and large-scale and low-frequency indices, such as the Southern Oscillation (SO) and the 40–50 day oscillation.

As from the geographical point of view the northern part of the African continent resembles the Australian region, a brief interhemispheric comparison of the cloudband over the Sahara and its Australian region counterpart is also presented.

2 Definitions and data sets

For the compilation of this TECB climatology we applied similar cloudband criteria as used in KUHNEL (1989). They specified that the TECB should:

a) have its origin between 40 °W–20 °E and 0°–20 °N (Fig. 3);
b) extend more than 25° in longitude;
c) have a maximum width of at least 5° latitude;
d) cross at least 10° of latitude;
e) have a more or less homogeneous texture (Fig. 1 a. 2).

The cloudband frequency has been expressed in terms of the number of days per month, rather than the number of the individual cloudbands per month. In this way, eventual difficulties in deciding whether to count one or two separate phenomena, when the system is reinforced through new surges of energy, have been avoided.

The results of this study are based on the following data sets:

a) daily TIROS-N/NOAA Series satellite infrared (IR) imagery, as published in Environmental Satellite Imagery (NOAA 1979–1983);
b) 3-hourly METEOSAT IR-imagery for the period April 28th–May 4th 1984;
c) mean monthly sea level pressure anomalies (MSLPAs) at 10 selected tropical stations (Fig. 3), based on data from the Monthly Climatic Data for the World (NOAA 1979–1983);
d) mean monthly sea surface temperature anomalies (SSTAs) for 4° squares between 32 °N and 32 °S, taken from NOAA National Meteorological Center SSTA set (Fig. 3).

As illustrated by Fig. 2 and mentioned later in the text, the TECB frequencies described in this paper are only valid in conjunction with the IR satellite channel. For correlations and power spectra the same

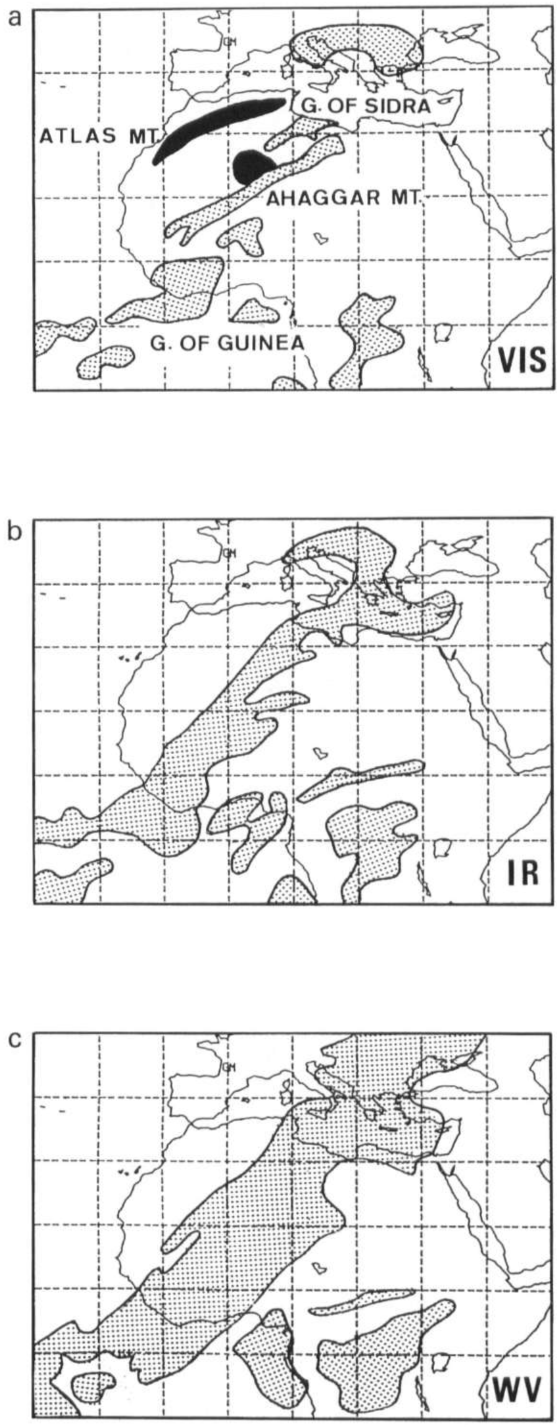

Fig. 2: Schematic illustration of a cloudband over the Sahara as seen in (a) visible (VIS), (b) infra-red (IR) and (c) water vapour (WV) METEOSAT2 channels on 30 April 1984 1200 GMT (black – major mountain ranges; stippled – TECB)

Schematische Abbildungen eines Wolkenbandes über der Sahara aufgenommen in drei verschiedenen (sichtbar, infrarot, Wasserdampf) METEOSAT-Kanälen

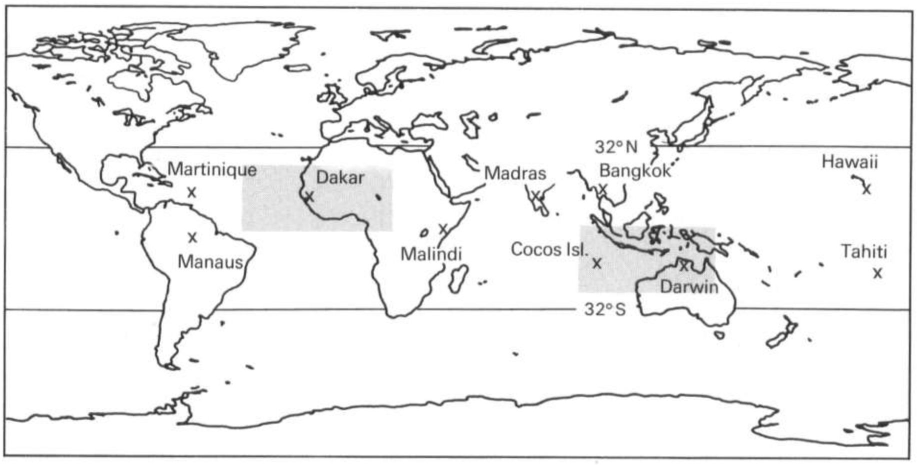

Fig. 3: Locations (outer limits) of the 10 selected MSLPA stations (tropical SSTAs) used in this study (areas of origin of the two respective cloudbands are shaded)

Standorte der 10 Stationen, deren Luftdruckwerte (bzw. äußere Grenzen der Gebiete, deren Meerestemperatur) in dieser Studie verwendet wurden

significance rules, as used in KUHNEL (1989), and described in MITCHELL et al. (1966), respectively, were applied.

3 *The cloudband over the Sahara in comparison with TECBs from other parts of the world*

As a number of previous studies (e.g. ANDERSON a. OLIVER 1970, FLOHN 1975, STRETEN 1973, THEPENIER 1981) have shown, the TECB over the Sahara does not represent the only axis along which tropical-extratropical exchange processes can take place. The latest work in this TECB series (KUHNEL 1989) actually indicates that, globally, we can distinguish between 14 such cloudbands, seven of them in each hemisphere. Thus, these cloudbands are rather common phenomena, which tend to develop in preferred locations in the outer tropics.

As their areas of development are generally defined by the positions of longwave mid-latitude upper level troughs and intertropical disturbances (e.g. FLOHN 1975, THEPENIER 1983), the Northern Hemisphere TECBs tend to form out of phase with their Southern Hemisphere counterparts. This is illustrated by figure 4, which also indicates that the cloudband over the Sahara has been observed on 312 days during the period 1979–1983. This total 5-year frequency ranks it as third amongst the Northern Hemisphere TECBs and sixth in a global intercomparison. Thus, the TECB over the Sahara does not belong to the most active cloudbands, but (together with the TECBs over East and South Africa and Australia) it is one of the few TECBs which lie predominantly over land.

As shown in figure 4 and described by KUHNEL (1989), globally, the most active cloudbands can be found over the central South Pacific and the eastern part of the South American continent (Note that no cloudbands originate over the tropical South Atlantic and the immediate vicinity of the western tropical South American coast).

4 *TECB structure and some synoptic aspects of its development*

Due to the scarcity of detailed meteorological data over the Sahara an extensive synoptic analysis of the TECB was not feasible. Nevertheless, FLOHN (1975) has indicated that the TECB over the Sahara usually develops ahead of a longwave mid-latitude upper level trough (reaching into subtropics), or in association with the Sahara depression. Similarly, THEPENIER (1981) suggested that the average climatological position of the TECB is closely connected with the Mediterranean zone of cyclogenesis. It seems though that a general low index circulation over the North Atlantic and an outbreak of cold polar air into low latitudes are rarely sufficient to cause a TECB development. As shown in figure 5, the probability of a TECB development increases with the establishment of a high latitude block, which has to form over the same longitudes as the cloudband origin and cause a general slow-down of the zonal circulation in

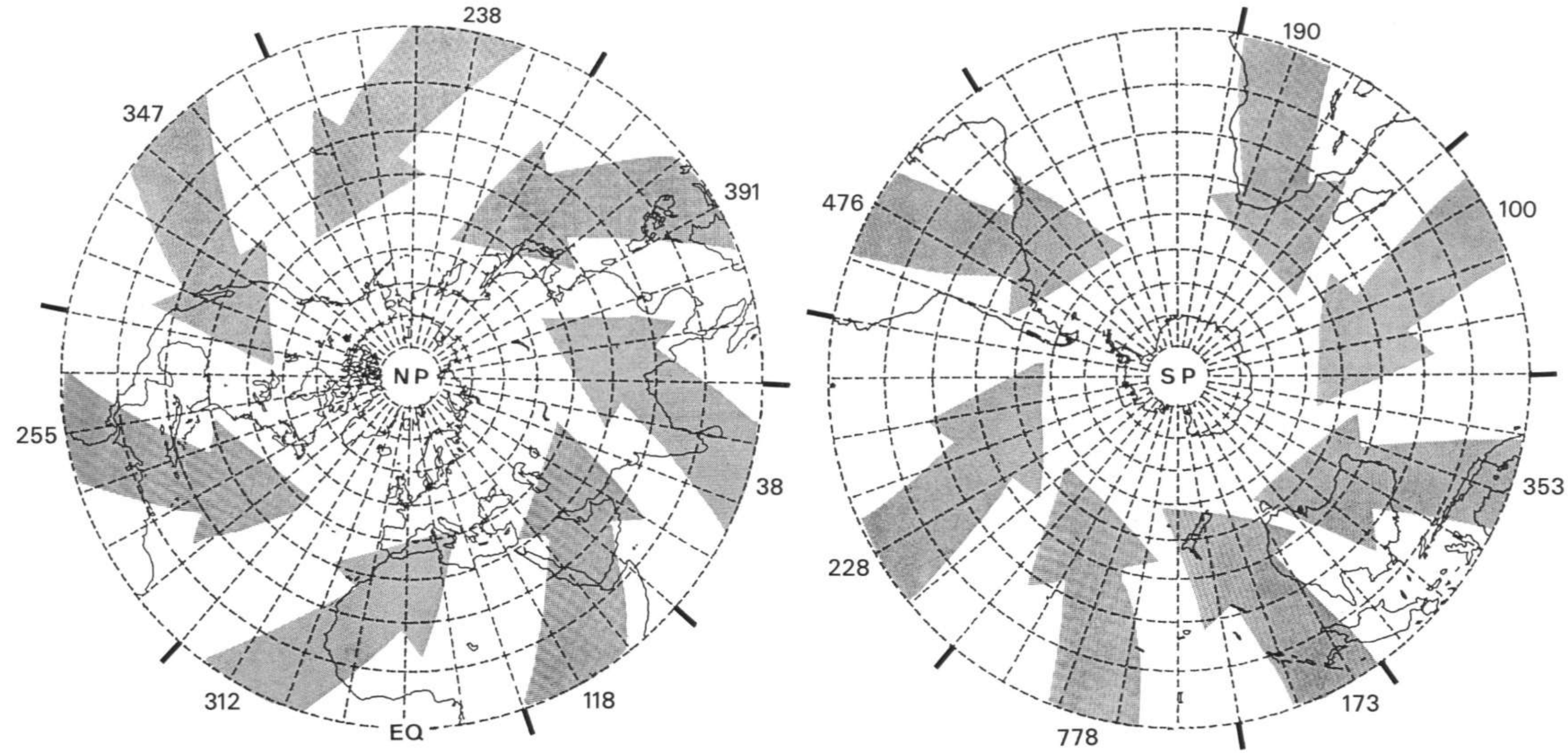

Fig. 4: Schematic illustration of the average climatological positions and total frequencies (in number of observation days) of 14 tropical-extratropical cloudbands for the period 1979–1983

Schematische Darstellung der mittleren klimatologischen Verbreitungsgebiete der 14 tropischen-extratropischen Wolkenbänder sowie deren Totalfrequenzen (in Tagen) für die Periode 1979–1983

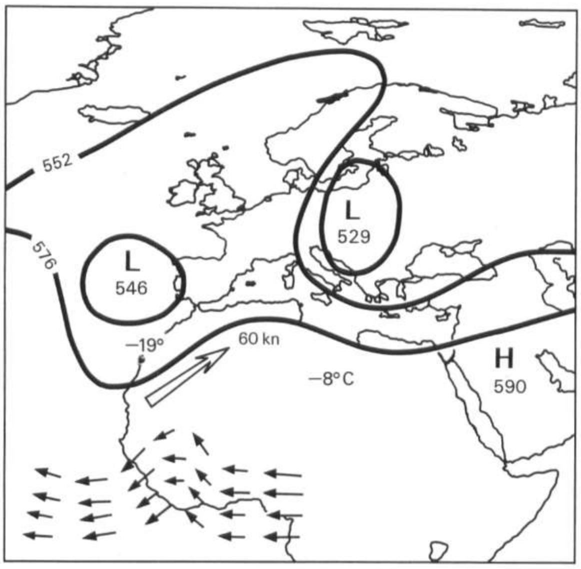

Fig. 5: Schematic illustration of typical atmospheric conditions on the initial day of the cloudband development (after ECMWF analyses for 27 April 1984) (bold lines show selected 500 mb height contours, bold arrows indicate the wind at 850 mb level, thin arrow and temperature values indicate the upper troposheric wind speed and 500 mb level temperature contrast developing over the consecutive 48 hours)

Schematische Darstellung der typischen atmosphärischen Bedingungen am Anfangstag einer Wolkenbandentwicklung

that region (Kuhnel 1987). Generally, a simultaneous development of a tropical disturbance, in the West African region often encountered in the form of an easterly wave (Fig. 5), is also necessary to inject more tropical moisture into the troposphere (e.g. Kuhnel 1987).

As a result of this configuration the temperature contrast between the Atlantic coast and central Sahara increases (Fig. 5) and the baroclinic zone over northwestern Africa becomes more pronounced (e.g. Kuhnel 1987). The associated tropospheric wind maximum, which generally shows a parallel alignment to the TECB, also increases (e.g. de Felice a. Viltard 1976; Fig. 5) and the warm and humid tropical air starts to slide up over the drier cold air, thus forming the actual TECB. Furthermore, the cloudband activity can be sustained for a longer period, if a cross-equatorial flow, which feeds more tropical moisture into the system, is present over the Gulf of Guinea (e.g. Kuhnel 1987; for orientation see Fig. 2a).

Examination of the METEOSAT satellite imagery shows that an average TECB over the Sahara displays the same basic structure, as described in some previous cloudband case studies from other parts of the world (e.g. Bell 1982, Tapp a. Barrell 1984). The highest clouds within the cloudband tend to be arranged along its sharp poleward edge near the poleward end, whereas its equatorward edge is rather diffuse (e.g. Fig. 1). This sloping structure across, as well as along the cloudband is characteristic for a well-developed TECB only, and is not necessarily visible in all cases. As the cloudband moves poleward and is about to reach the mid-latitude westerlies, the curvature of its poleward end becomes more anticyclonic, and it starts to dissipate due to the subsiding air ahead of it (Fig. 1). Occasionally, the cloudband can merge and interact with an extratropical front, causing moderate to heavy rainfall over Northern Africa and the Mediterranean (e.g. Winstanley 1970). Though (due to the scarcity of detailed data) the capacity of the TECB to produce rain was not examined here in detail, the work of Smith a. Sohn (1990) indicates that, over North Africa, a strong relationship exists between monthly rainfall figures and monthly mid-cloud amounts. Considering that the TECB (one of the major causes of cloud anomalies over central Sahara during the winter months) tends to develop at the mid-tropospheric level (Kuhnel 1987), it seems that the TECB is also likely to play a substantial role in the cloud amount-rainfall relationship.

5 TECB frequency and duration

Figure 6a shows the monthly numbers of TECB days for the period January 1979–December 1983. The curve reveals that the cloudband over the Sahara is basically a northern winter phenomenon. As shown in table 1, the cloudband reaches its maximum frequency in the month of March. This is in agreement with the results of Thepenier (1983), though she subdivided this cloudband into four smaller categories and her area of TECB origin extended further west. The reason for the subdivision may have been the relatively strong seasonal changes of the TECB alignment, also noted by Stucki (1983).

A direct comparison with the results of Thepenier (1981, 1983) is not possible, as she does not list the annual TECB frequencies, but her results are likely to be slightly different due to the choice of the TECB area of origin. When checked against the results of Stucki (1983), frequencies presented here show substantially lower TECB numbers for the period October 1981–September 1982 (28 cases against 36

Table 1: Total annual and mean monthly frequencies for the TECB over the Sahara
Jahres- und Monatsfrequenzen des Wolkenbandes über der Sahara

	Year:		1979		1980		1981	1982		1983		
	TECB days:		63		53		49	87		60		
Month:	Jan	Feb	Mar	Apr	May	Jun	Jul	Aug	Sep	Oct	Nov	Dec
TECB days:	8.2	7.2	8.8	8.2	4.6	1.0	0.0	0.0	1.0	8.4	7.0	8.0

cases counted by Stucki). This difference of 25 percent can be attributed to the use of different spectral channels (see also Fig. 2). In fact, the major differences with the water vapour channel statistics of Stucki were found to occur during the summer months (June–August), when no cloudbands appear in the IR-imagery.

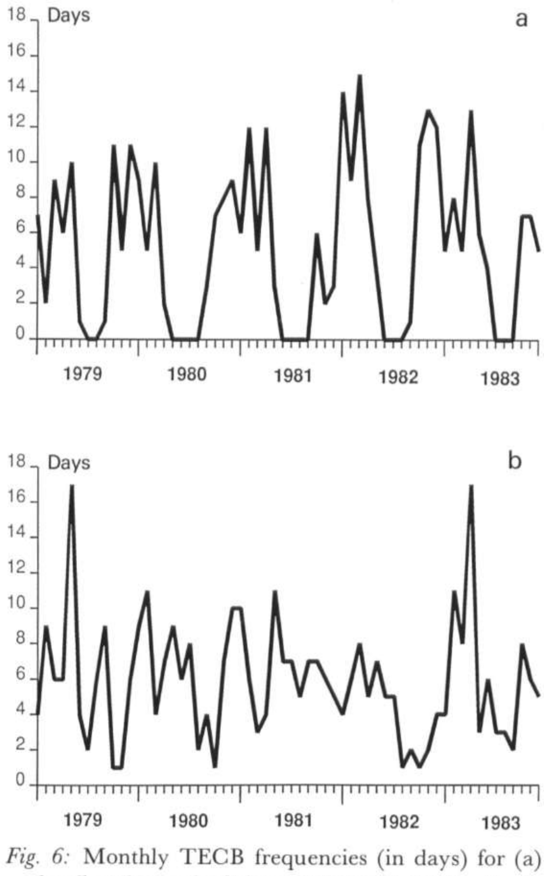

Fig. 6: Monthly TECB frequencies (in days) for (a) the cloudband over the Sahara (TECB S), (b) the cloudband in the Australian region (TECB A) for the period 1979–1983

Monatsfrequenzen (in Tagen) des Wolkenbandes über der Sahara (a) sowie des Wolkenbandes über Australien (b) für die Periode 1979–1983

Most of the cloudbands over the Sahara are not very long-lived features, with roughly 40 percent of them lasting for one day only. Longer durations up to 9 days are possible, though they are quite rare, as the average TECB duration of 1.9 days suggests. The stronger cloudbands can cross the whole northern part of the African continent and interact with an extratropical front in the Mediterranean. According to Thepenier (1983), this happens in roughly 50 percent of TECB cases.

6 TECB activity and atmospheric pressure in the tropics

In order to examine potential links between the TECB activity and sea level pressure fluctuations in the tropics we cross-correlated the monthly TECB frequency anomalies with the monthly MSLPAs at various tropical locations (Fig. 3). In contrast to the global TECB study (Kuhnel 1989), the correlations have been extended to lag −6 and +6 months. Although the analysis resulted in a couple dozen of significant correlations, the discussion in the following sections concentrates only on the most significant ones.

As a monthly stratification of the data was not feasible (due to the relatively short period of investigation) the coefficients of correlations (CCFs), shown in figure 7, are relatively low. Nevertheless, they seem to indicate that, with a delay of 2–3 months, the TECB activity is likely to respond positively to anomalous MSLP changes over the eastern Indian Ocean-Australian region, and negatively to MSPLAs from the western North Atlantic Ocean. Whereas the link with the eastern Indian Ocean might partly reflect the signal of the Southern Oscillation (as discussed later), the connection to the western North Atlantic seems to be more relevant in this context. As shown by Liebmann a. Hartmann (1984), reverse pressure conditions over the western and eastern halves of the North Atlantic Ocean, which are favourable for the TECB development, are not uncommon on a shorter time scale (5–10 days).

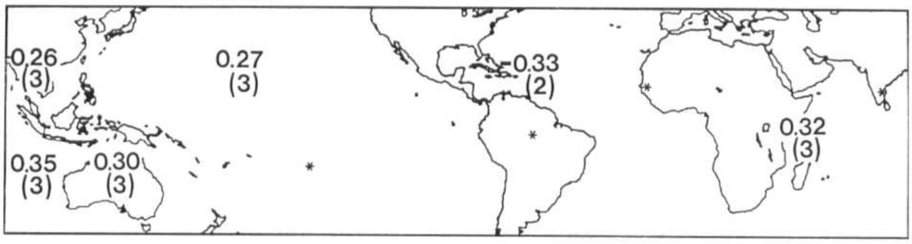

Fig. 7: Plot of selected highest significant correlation coefficients between MSLPAs at selected tropical stations and frequency anomalies of the TECB over the Sahara (95% significance level used, numbers in parantheses indicate lag in months - MSLPA leads TECB)

Die höchsten (statistisch signifikanten) Korrelationskoeffizienten zwischen den Luftdruckanomalien der 10 ausgewählten Stationen und den Frequenzanomalien des Wolkenbandes über der Sahara

On the other hand, the TECB development is also likely to be controlled by teleconnection processes with regions located upstream. As the CCF of −0.33 (with MSLPA at Martinique at lag +2) in figure 7 suggests, the TECB activity in November–January is likely to be negatively coupled with the pressure conditions in the Caribbean region during the preceding hurricane season. This does not necessarily mean that the TECB development is also linked with the number of hurricanes in the Caribbean, as the latter has been shown to be related to the Southern Oscillation Index (SOI), but often MSLPA independent (GRAY 1984).

The positive significant correlation coefficient with the MSLPA at Cocos Island at lag 3 (Fig. 7) does suggest that a stronger TECB activity is preceded by an unusually high pressure over Australo-Indonesia during the (southern) winter months. Furthermore, the results of correlations with the MSLPAs at Darwin and Tahiti reach the significance level a second time at lag+2 and lag+4 months respectively (not shown). As their CCFs display different signatures (positive with the MSLPA at Darwin and negative with the MSLPA at Tahiti), they suggest a positive relationship between warm ENSO (El Nino-Southern Oscillation) events and TECB activity.

7 *TECB activity and tropical sea surface temperature*

To establish the relationship between the TECB activity and tropical/subtropical sea surface temperature anomalies these two parameters have again been cross-correlated between lag−6 and lag+6 months. Despite the fact that the areas with significant CCFs resulting from the correlations between the TECB frequency anomalies and the SSTAs are generally small and scattered over all major oceans, it seems possible to link a few of them more closely with the TECB development.

As a general rule, it can be said that the correlations do result in negative CCFs from lag+1 to lag+6 months (SSTA leading TECB activity) and positive CCFs from lag−1 to lag−6 months (SSTA lagging TECB activity). This overall pattern does, at least partly, reflect the signal of the 1982/1983 ENSO. An exception to this rule is a relatively large area of positive CCFs appearing in the western Indian Ocean north of Madagascar at lag 3 and 4 (Fig. 8a). It indicates that an anomalous SST increase (decrease) in the western Indian Ocean is likely to be followed by anomalous increase (decrease) in TECB activity 3–4 months later. In addition, this pattern suggests a link between the strength of the Indian monsoon and the TECB activity, as it is located over the western edge of the monsoonal circulation.

As mentioned in KUHNEL (1989), the anomalous SST changes, which occur in the eastern North Atlantic one month prior to anomalous TECB activity (Fig. 8b), seem to represent one of the more important TECB precursors. Using the assumption that the eastern North Atlantic SST pattern is forced by atmospheric pressure (LOUGH 1986), the anomalous SST changes off the western North African coast are likely to reflect the higher frequency of autumnal surges of cold extratropical air masses into low latitudes. As shown in the *United States Navy Marine Climatic Atlas of the World* (1974) climatology, a combination of a weak autumnal Azores High over the central North Atlantic with simultaneous strengthening of the Icelandic Low may also enhance the intensity of these cold surges.

Concurrently, the coastal and shelf areas of this part of the North Atlantic are also dominated by wind-driven upwelling, which, south of 20° N, is most dominant during the winter and spring months

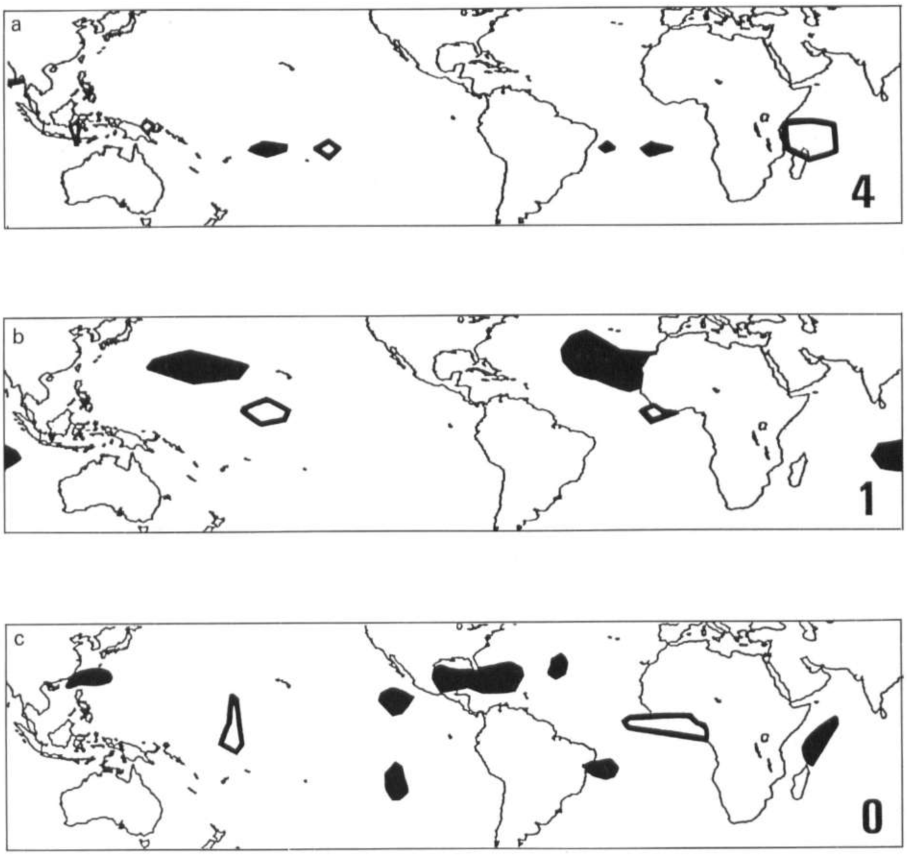

Fig. 8: Plots of significant correlation coefficients between tropical SSTAs and frequency anomalies of the TECB over the Sahara at (a) lag 4 months (SSTA leads TECB), (b) lag 1 month, (c) lag 0 month (black/white (enclosed by bold lines) areas with negative/positive correlation coefficients significant at the 95% level)

Gebiete mit signifikanten Korrelationskoeffizienten zwischen den Meerestemperaturanomalien und den Frequenzanomalien des Wolkenbandes über der Sahara

(MITTELSTAEDT 1991). This results in relatively low SSTs, which, under the influence of a cyclonic gyre (occuring off the Northwest African coast between 15° N and 20° N throughout the year, (MITTELSTAEDT 1991)), can spread as far as 300 kilometers offshore (compare with Fig. 8b). Moreover, during the spring season, a strong meridional SST gradient generally develops around 15° N, as a tongue of warm surface water (> 26° C) starts to spread from the open ocean towards the equatorial West African coast. According to MITTELSTAEDT (1991), this water mass, which dominates the TECB area of origin during its maximum of activity (Table 1), represents the seasonal advance of tropical water with the North Equatorial Counter Current (NECC). Consequently, the associated development of a zone of strong SST gradient is likely to enhance the production of atmospheric eddies over the area of TECB origin. These eddies are known to play an important part in the meridional transport of tropical heat, moisture and momentum.

This overall correlation pattern is later (at lag 0) followed by a configuration with positive CCFs in the Gulf of Guinea and negative CCFs over the western part of the North Atlantic Ocean (Fig. 8c). Once again, this pattern seems to be the result of atmospheric forcing during the mature ENSO phase (CAC/WMC-Washington 1982–1984). As a consequence of it, many cloudbands form further west over the Atlantic Ocean (or east over central and eastern Africa) and do not cross the central Sahel or Sahara (KUHNEL 1987). This is in agreement with the results of other studies (e.g. LAMB 1978, BAH 1987), which indicate that dry years in the Sahel are often characterised by the presence of warm waters in the Gulf of Guinea.

8 TECB activity and the Southern Oscillation

Figure 9 displays the CCFs between monthly TECB frequency anomalies and the Southern Oscillation Index (here defined as MSLPA at Tahiti minus MSLPA at Darwin) for lag-12 to lag+12 months. The CCF curve, which reaches the significance level between lag-2 and lag-4 months (TECB activity leading the SOI), suggests that the TECB activity is likely to increase shortly prior to the mature phase of a warm ENSO event. Despite the fact that this result loses its significance, when the persistence of the SO index is considered (GREENHUT 1979), the above mentioned negative relationship between the TECB activity and the SOI is supported by the CCF results with MSLPAs and SSTAs (described in previous two sections). A similar, but somewhat weaker trend, can also be found at lag+3 months and lag +5 months (Fig. 9).

Nevertheless, due to a complex relationship between satellite observed cloud cover and precipitation amounts (RICHARDS a. ARKIN 1981), as well as fluctuations in TECB trajectories (STUCKI 1983, KUHNEL 1987), the above mentioned TECB tendency may not necessarily be reflected in rainfall figures over the Sahara or the Sahel. In fact, the Sahel region experienced a period of severe drought commencing in 1982 (e.g. CAC/WMC-Washington 1982-1984).

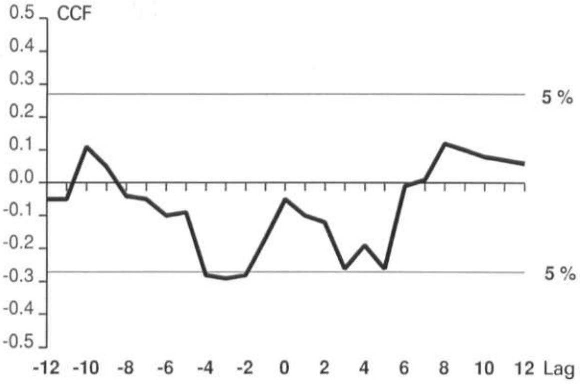

Fig. 9: Correlation coefficients between frequency anomalies of the TECB over the Sahara and the Southern Oscillation Index for lag -12 months to lag +12 months (95% significance level used; negative/positive lag indicates TECB leads/lags SOI)

Korrelationskoeffizienten zwischen den Frequenzanomalien des Wolkenbandes über der Sahara und dem „Southern Oscillation Index“ (Luftdruckanomalie-Differenz zwischen den Stationen Darwin und Tahiti)

9 TECB activity and various pressure difference indices

Despite the previously discussed trend between TECB activity and the Southern Oscillation Index, Western Africa does not belong to the few regions on Earth, which show a strong SO signal (e.g. ROPELEWSKI a. HALPERT 1987). For this reason, the author has created other pressure indices using MSLPA differences between pairs of 10 selected tropical stations (Fig. 3), with the hope that some of them might lead to better correlation coefficients than the SOI, which, in this case, is not a very useful predictor.

As shown in figure 10, this assumption proved right. Especially the index MSLPA at Cocos Island minus MSPLA at Martinique leads to a higher CCF (of 0.34 at lag +2) than the actual SOI. Nevertheless, the relationships depicted bear certain ENSO characteristics, as the two dipoles of the North Australian - Caribbean region index are known to be linked by teleconnection processes (REITER 1983), and the TECB area of origin is connected with the Caribbean via the cross-Atlantic index (MSLPA at Martinique minus MSLPA at Dakar).

10 TECB activity and low-mode oscillations

Since MADDEN a. JULIAN (1971) first found a well-defined 40-50 day peak in the variance spectrum of the tropospheric winds at Canton Island, the activity of several other meteorological parameters has been reported to follow a similar pattern (e.g. KRISHNAMURTI et al. 1985, MURAKAMI a. NAKAZAWA 1985). Later, LAU a. CHAN (1986) suggested that this 30-40 day (e.g. YASUNARI 1980), or 30-60 day (e.g. KNUTSON et al. 1986) oscillation mode could be related with the ENSO events. As the TECB activity shows a weak relationship with the ENSO, it was interesting to see if it also displays any dominant low-mode oscillation (in the 30-60 day range).

The result of a Fourier analysis applied to the whole 5-year time series of TECB frequency is rather inconclusive, showing only an insignificant amplitude peak in the range of 21-64 days (not shown). This is not surprising considering the strong annual cycle of the TECB frequency data (Fig. 6a, Table 1). On the other hand, the results show a somewhat clearer pattern, if the 5-year time series is subdivided, and the analysis is applied to segments with the length of 128 days (starting with dates January 1st, April 1st, and September 1st).

The strongest significant amplitudes resulted from the analysis of segments commencing in January, and

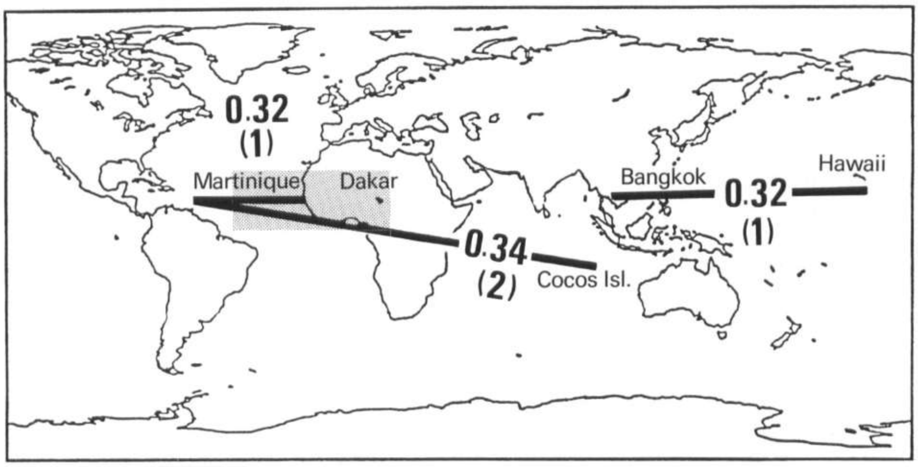

Fig. 10: Selected MSLPA indices showing the highest significant correlation coefficients with frequency anomalies of the TECB over the Sahara (99% significance level used; numbers in parantheses below the CCF indicate lag in months - MSLPA leads TECB)

Indizes der Luftdruckanomalie-Differenz, die zu den höchsten statistisch signifikanten Korrelationskoeffizienten mit den Frequenzanomalien des Wolkenbandes über der Sahara führen

were associated with periods ranging from 12 to 25 days. An example of this type of power spectrum is shown in figure 11. This periodicity (around 20 days) resembles roughly the quasi-periodical 3-6 week oscillation of the "zonal index" (defined as the strength of zonal midlatitude westerlies at 700 mb) first described by NAMIAS (1950). Similarly, it also matches the 24-periodicity reported to occur in hemispheric-scale energy parameters during the winter months (McGUIRCK a. REITER, 1976).

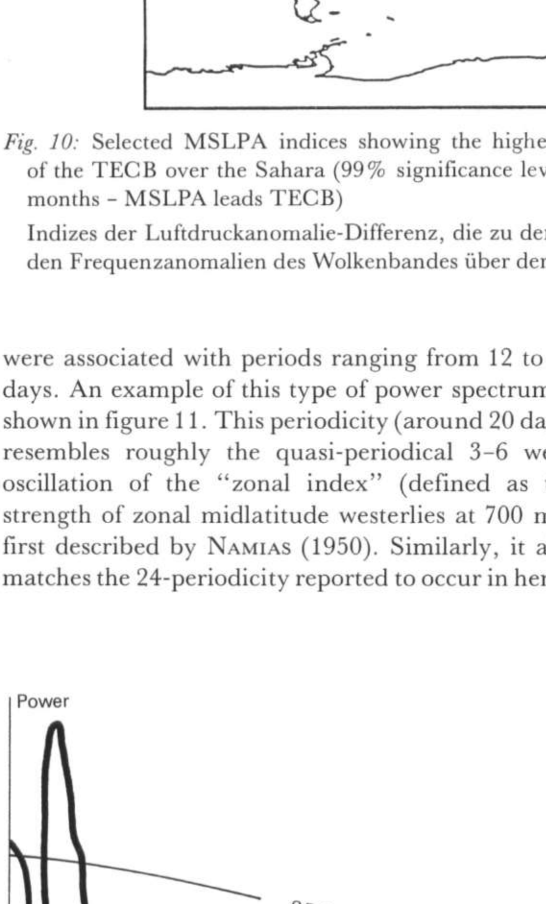

Fig. 11: Typical power spectrum of (winter) TECB over the Sahara frequency, showing a maximum periodicity of roughly 20 days (based on the time series of 128 days starting on January 1st 1979)

Typische Spektralkurve der Wolkenbandfrequenz mit einem signifikanten Periodizitätsmaximum von etwa 20 Tagen

In contrast, the analysis of the time series segments covering the spring and summer months (128 days starting on April 1st) showed only very weak amplitudes peaking at a period of 64 or 128 days. This low-mode periodicity seems to reflect the 3-4 months long summer period, which is actually marked by the absence of TECB activity.

With the exceptions of winter 1980/1981 and the beginning of 1983, when the cloudband development was marked by a strong (significant) 32-day and (not significant) 64-day periodicity, respectively, the fluctuations in the TECB actually never reflected the 40-50 day (or 30-60 day) oscillation, observed in other parameters over other parts of the world.

11 Comparison of the TECB over the Sahara and its counterpart in the Australian region

From the geographical and the climatological points of view the cloudband over the Sahara (TECB S) and the cloudband developing northwest of Australia (TECB A) have several aspects in common. Both originate over tropical waters west of a major continent (Fig. 3), and both extend over large arid areas into the middle latitudes. Embedded between two monsoon or monsoon-like systems (the Southeast-Asian and Australian monsoons for the TECB A/West African monsoon and the Amazon basin for the TECB S), their origins are located over moderately warm equatorial sea currents, with sea surface temperatures exceeding 25 °C. Furthermore, both originate equatorward of a major quasi-permanent upper level trough (e.g. Flohn 1975), close to or over the boundary of the Intertropical Convergence Zone (ITCZ).

In contrast to the TECB S, which is a winter phenomenon (Fig. 6a), the TECB A shows a more complicated frequency distribution (Fig. 6b). This is partly due to tropical cyclone activity, which influences Northern Australia, but is absent in the West African region. The slightly higher number of TECB A observations during the period 1979–1983 (353 and 312 respectively) can probably be attributed to TECB A development from tropical cyclones. On the other hand, the total frequencies of both cloudbands take third place in their individual hemispheric TECB frequency rankings (Fig. 4).

As mentioned before and discussed in Kuhnel (1990), the beginning of the respective cloudband development is generally associated with an intrusion of cold air masses into low latitudes and a temporary establishment of a mid-latitude block at the longitude of the TECB origin. In the case of TECB S, the development can also be initiated by the Sahara depression, forming in lee of the Atlas mountains (Flohn 1975). These processes, sometimes combined with tropical forcing of atmospheric or oceanic origin (Kuhnel a. Henderson-Sellers 1991), lead to deepening of the baroclinic zone over the respective areas of TECB development. In contrast to the TECB related tropical forcing in the Australian region, which can generally be associated with an extension of the Southeast-Asian monsoon depression system or a tropical cyclone, the intertropical disturbances in the West African region are often encountered in the form of easterly waves.

A comparison of their development scenarios (e.g. Bell 1982, Tapp a. Barrell 1984, Flohn 1975, Kuhnel 1990) has shown that both TECBs are very similar. Although both TECBs show the same basic sloping structure along (across) the cloudband, TECB A cases are often more homogeneous than TECB S phenomena, which can sometimes become distorted after the passage of the Atlas and/or Ahaggar mountains. In some cases the high mountain ranges can actually block a further TECB S development, which is partly reflected in shorter average TECB S duration (1.9 days for TECB S and 2.6 days for TECB A respectively; Kuhnel 1990) and a lower percentage of TECB S phenomena merging with an extratropical front (50% and 64% respectively; Thepenier 1983, Kuhnel 1990). The longer average duration of TECB A can also be partly attributed to the cross-equatorial flow, which is somewhat stronger in the Australo-Indonesian region than over western equatorial Africa.

Being situated in the vicinity of the western pole of the Southern Oscillation, TECB A also responds earlier and stronger then TECB S to warm ENSO events. Whereas the TECB A development is definitively supressed 5–6 months prior to the mature ENSO event (Kuhnel 1990), the TECB S activity seems to be slightly enhanced by the same process. As suggested in Kuhnel (1990), the TECB A activity shows a more or less well-defined 40–50 day oscillation during warm ENSO events, whereas no such fluctuations in the TECB S development can be observed in the North African region. As mentioned earlier, the most dominant TECB S oscillation mode can be associated with the period of 12–25 days, an oscillation also commonly associated with the "zonal index cycle", as well as the vacillation of atmospheric parameters in the Northern Hemisphere during the winter months. A similar oscillation pattern is also common for the TECB A activity during seasons with positive SOI (Kuhnel 1987).

12 Conclusions

In this study the author has investigated the characteristics of tropical-extratropical cloudband development over the Sahara by linking it to the activity of other meteorological parameters, like tropical MSLPAs, SSTAs, SOI and other low-mode oscillation indices. The major results of this climatology indicate that the TECB over the Sahara is a well-defined northern winter phenomenon, whose activity peaks in March and is likely to show:

- positive lagged (3 months) response to anomalous MSLP changes over the eastern South Indian Ocean, and negative lagged (2 months) response to MSLPA at Martinique;
- positive lagged (3–4 months) response to anomalous SST changes in the western Indian Ocean (northeast of Madagascar), negative lagged (1 month) response to SSTAs in the eastern North Atlantic, as well as a simultaneous positive reaction to SSTAs in the Gulf of Guinea. The latter two signals seem to be of major importance for the cloudband development.

Furthermore, the results suggest that the TECB activity is likely to increase prior to the mature phase of warm ENSO events, as well as to show a well-defined lagged (2–3 months) positive relationship with cross-Atlantic and Australian-Caribbean region pressure indices (e.g. MSLPA at Dakar - MSLPA at Martinique, MSLPA at Cocos Island - MSLPA at Martinique). Fourier analysis of segmented (128 days) TECB time series indicates that during the January-March period the TECB development shows a significant oscillation with a period of roughly 20 days. This fluctuation resembles closely the oscillation period generally associated with the (Northern Hemisphere) "zonal index".

A comparison between the cloudbands from the North African and Australian regions revealed that the cloudbands are similar in many respects. They both show the same basic sloping structure (with a sharp poleward edge running parallel to a stronger subtropical wind maximum and diffuse equatorward edge), as well as similar general synoptic patterns accompaning their development (e.g. intrusion of cold air into low latitudes, eventual block development, presence of tropical disturbance and baroclinic zone).

Nevertheless, some regional differences were noticed. It seems that the North Atlantic cold surges have to be somewhat stronger (than those in the eastern South Indian Ocean) in order to trigger off a TECB development. This may be due to the fact that the northern winter tropical disturbances over West Africa (another important aspect of the TECB development) are somewhat less vigorous, but more mobile, than those in the eastern South Indian Ocean. They are often encountered in the form of easterly waves which are rather uncommon in the Australo-Indonesian region. On the other hand, no tropical cyclones, from which a TECB could develop, are encountered in the Gulf of Guinea. Similarly, cross-equatorial flow, which can prolong the TECB activity through a sustained supply of moisture, is not observed as often in the West African as in the Australo-Indonesian region. This fact is partly reflected in a longer average duration of TECB events over Australia than those over the Sahara. Furthermore, the formation of many TECBs over the Sahara can be triggered off, or enhanced by, the formation of a Sahara depression, which develops partly due to orographic forcing (by the Atlas mountains), and thus has no counterpart in the West Australian region.

Considering the relatively large importance these cloudbands can have on the marginal precipitation regime over generally arid areas, the TECB climatology should be extended over a much longer period. As these cloudbands can easily help visualise the main axes of exchange processes between the tropics and extratropics, their extended climatology could point to any anomalous changes, which have occured in the general circulation over the past three decades, and thus benefit the current Greenhouse Effect research.

Acknowledgements

I thank Dr. T. T. Gibson from the Meteorology Department of the University of Melbourne, who supervised and guided this study for most of the time. I also thank Prof. M. Winiger from the University of Bonn, who provided additional satellite imagery used in this work. The final touches to this manuscript would not have been possible without the support of an Australian Research Council grant, which is herewith gratefully acknowledged.

References

ANDERSON, R. K. a. OLIVER, V. J.: Some examples of the use of synchronous satellite pictures for studying changes in tropical cloudiness. In: Proc. Symp. on Tropical Meteorology, Hawaii, 1970.

BAH, A.: Towards the prediction of Sahelian rainfall from sea surface temperatures in the Gulf of Guinea. In: Tellus 39, 1987, 39-48.

BELL, I. D.: Extratropical cloud systems: Satellite interpretation and three dimensional airflows. Unpublished Ph. D. Thesis, Monash University, 1982.

CADET, D. L. a. NNOLI, N. O.: Water vapor transport over Africa and the Atlantic Ocean during summer 1979. In: Q. J. R. Meteorol. Soc. 113, 1987, 581-602.

Climate Analysis Center (CAC), WMC-Washington: Monthly Climate Diagnostic Bulletins, 1982-1984.

DE FELICE, P. a. VILTARD, A.: Aérojet subtropical d'hiver et nuages associés. In: La Météorologie, VI[e] Serie 6, 1976, 223-225.

DUBIEF, J.: Le climat du Sahara. Mémoires I. R. S., Vol. 1, 1959

DUBIEF, J. a. QUENEY, P.: Les grands traits du climat du Sahara Algérien. In: La Météorologie 119, 1935, 80-91.

FLOHN, H.: Tropische Zirkulationsformen im Lichte der Satelliten-Aufnahmen. Bonn. Met. Abhand. 21, 1975.

GRAY, W. M.: Atlantic seasonal hurricane frequency. Part I: El Niño and 30 mb quasi-biennial oscillation influences. In: Mon. Wea. Rev. 112, 1984, 1649-1668.

GREENHUT, G. K.: 'Reply'. In: J. Phys. Oceanogr. 9, 1979, 1298-1299.

KNUTSON, T. R., WEICKMANN, K. M. a. Kutzbach, J. E.: Global-scale intraseasonal oscillations of outgoing longwave radiation and 250 mb zonal wind during Northern Hemisphere summer. In: Mon. Wea. Rev. 114, 1986, 605-623.

KRISHNAMURTI, T. N., JAYAKUMAR, P. K., SHENG, J., SURGI, N. a. KUMAR, A.: Divergent circulation on the 30-50 day time scale. In: J. Atmos. Sci. 42, 1985, 364-375.

KUHNEL, I.: Bewölkung, Niederschlag und atmosphärische Zirkulation in Ostafrika. In: Berner Beiträge zur Afrikaforschung, Jahrbuch der Geogr. Gesellschaft von Bern 54/80-82, 1983, 139-159.

– : Tropical-extratropical cloudband climatology based on satellite data. Ph. D. Thesis, Melbourne University, 1987.

– : Tropical-extratropical cloudband climatology based on satellite data. In: Int. J. Climatol. 9, 1989, 441-463.

– : Tropical-extratropical cloudbands in the Australian Region. In: Int. J. Climatol. 10, 1990, 341-364.

KUHNEL, I. a. HENDERSON-SELLERS, B.: Mixed layer modelling with respect to ocean-atmosphere interactions in the eastern Indian Ocean. In: Met. and Atmos. Physics 46, 1991, 51-64.

LAMB, P. J.: Large-scale tropical Atlantic surface circulation patterns associated with sub-Saharan weather anomalies. In: Tellus 30, 1978, 240-251.

LAU, K. M. a. CHAN, P. H.: The 40-50 day oscillation and the El Nino/Southern Oscillation: A new perspective. In: Bull. Amer. Meteorol. Soc., 67, 1986, 533-534.

LIEBMANN, B. a. HARTMANN, D. L.: An observational study of tropical-midlatitude interactions on a intraseasonal time scale during winter. In: J. Atmos. Sci. 41, 1984, 3333-3350.

LOUGH, J. M.: Tropical Atlantic sea surface temperatures and rainfall variations in sub-Saharan Africa. In: Mon. Wea. Rev. 114, 1986, 561-570.

MADDEN, R. A. a. JULIAN, P. R.: Detection of a 40-50 day oscillation in the zonal wind in the tropical Pacific. In: J. Atmos. Sci. 28, 1971, 702-708.

MCGUIRCK, J. P. a. REITER, E. R.: A vacillation in atmospheric energy parameters. In: J. Atmos. Sci., 33, 11, 1976, 2079-2093.

MITCHELL, J. M., DZERDZEEVSKII, B., FLOHN, H., HOFMEYER, W. L., LAMB, H. H., RAO, K. N. a. WALLEN, C. C.: Climatic Change, Technical Note No. 79, WMO, Geneva 1966.

MITTELSTAEDT, E.: The ocean boundary along the northwest African coast: circulation and oceanographic properties at the sea surface. In: Prog. Oceanogr. 26, 1991, 307-355.

MURAKAMI, T. a. NAKAZAWA, T.: Tropical 45 day oscillations during the 1979 Northern Hemisphere summer. In: J. Atmos. Sci. 42, 1985, 1107-1122.

NAMIAS, J.: The index cycle and its role in the general circulation. In: J. Meteor. 7, 1950, 130-139.

NOAA, U. S. Department of Commerce: Environmental satellite imagery (Key to meteorological records documentation No. 5.4). NOAA, 1979-1983.

NOAA, U. S. Weather Bureau: Monthly Climatic Data for the World. National Climatic Center, Asheville, NC, 1979-1983.

REITER, E. R.: Teleconnections with tropical precipitation surges. In: J. Atmos. Sci. 40, 1983, 1631-1647.

RICHARDS, J. a. ARKIN, P.: On the relationship between satellite observed cloud cover and precipitation. In: Mon. Wea. Rev. 109, 1981, 1081-1093.

ROPELEWSKI, C. F. a. HALPERT, M. S.: Global and regional scale precipitation patterns associated with the El Niño/ Southern Oscillation (ENSO). In: Mon. Wea. Rev. 114, 1987, 2352-2362.

SMITH, E. A. a. SOHN, B. J.: Surface forcing of interannual variations in the radiation balance over North Africa. Part I: Partitioning the surface and cloud forcing. In: Clim. Change 17, 2-3, 1990, 147-192.

STRETEN, N. A.: Some characteristics of satellite observed bands of persistent cloudiness over the Southern Hemisphere. In: Q. J. R. Meterol. Soc. 99, 1973, 56-73.

STUCKI, J. P.: Der Austausch: Tropen Ektropen in der Sicht der Wasserdampfbilder von METEOSAT I und II. Unpublished M. Sc. Thesis, University of Berne, 1983.

TAPP, R. G. a. BARRELL, S. L.: The Northwest Australian cloud band: Climatology, characteristics and factors associated with development. In: J. Climatol. 4, 1984, 411-424.

THEPENIER, R. M.: Étude climatologique des bandes nuageuses pour l'ensemble de l'hémisphère nord. In: Météorologie, VI[e] Serie 25, 1981, 61-68.

– : Étude des perturbations nuageuses de l'hémisphère nord: rôle de la convection dans la cyclogenèse. Ph. D. Thesis, L'Université Pierre et Marie Curie, Paris, 1983.

United States Navy: U. S. Navy Marine Climatic Atlas of the World, North Atlantic Ocean, Vol. 1. Naval Weather Service Detachment, Asheville, NC, 1974.

WINIGER, M.: Bewölkungsuntersuchungen über der Sahara mit Wettersatellitenbildern. Geographica Bernensia, G1, 1975.

WINSTANLEY, D.: The North African flood disaster September 1969. In: Weather 25, 1975, 390-403.

YASUNARI, T.: A quasi-stationary appearence of a 30-40 day period in the cloudiness fluctuations during the summer monsoon over India. In: J. Met. Soc. Jap. 58, 1980, 225-229.